Dan Wu, Fuming Wang*, Jin Cheng and Changrong Li

Effect of Nb and V on Austenite Grain Growth Behavior of the Cr-Mo-V Steel for Brake Discs

https://doi.org/10.1515/htmp-2017-0077
Received June 1, 2017; accepted January 2, 2018

Abstract: In order to improve the performance of the steel for brake discs, including strength, toughness and thermal fatigue resistance, Nb and V are added to the steel. The effect of Nb and V on austenite grain growth behavior of the Cr-Mo-V steel for brake discs was studied by analyzing the phase equilibria as well as the microstructures. The precipitation behaviors of precipitates were also investigated based on transmission electron microscopy and energy-dispersive spectroscopy. The results showed that V-rich M_8C_7 and NbC particles existed at the experimental temperatures. The abnormal grain growth in Nb-free steels was affected by the partial dissolution and coarsening of M_8C_7 particles. With increasing V content, the grains were refined, but the mixed grain phenomenon became more serious. There were many small NbC particles in Nb-bearing steel, so the grains were effectively refined. Furthermore, a prediction model, which calculates the austenite grain size considering precipitate pinning effect, was established, and the model was well consistent with the actual situation in the Nb-bearing steel up to 1,100 °C. The grains of the Nb-free steels were sensitive to the increments of temperature and time due to the rapid dissolution or coarsening of M_8C_7 particles.

Keywords: brake disc steel, vanadium, niobium, austenite grain, precipitate growth

Introduction

The brake disc is an important safety component of railway vehicles. During the braking process, the kinetic energy is converted into heat through the violent friction between the brake disc and the pad. The brake disc absorbs most heat and only a little energy is emitted into the air [1, 2]. Compared to ordinary train, the high-speed train has a much faster speed and the greater braking energy is generated under hard braking. Under such conditions, the temperature of the brake disc increases rapidly, and the peak temperature may exceed the A_3 temperature [3]. The drastic temperature change causes high thermal stress and the austenite transformation results in microstructure stress. After repeated braking cycles, cracks will be generated on the friction surface of the brake disc due to the thermal and the microstructure stresses [4, 5]. Therefore, a higher requirement is suggested for the material used as brake discs [6].

The Cr-Mo-V steel for brake discs is an alloy steel which needs quenching and tempering heat treatment, and its performance, including strength, toughness, wear resistance and heat resistance, is excellent [7]. In general, the properties of steels are closely related to alloying elements. The additions of Cr and Mo improve the strength of steels by solid solution strengthening and precipitation strengthening effects [8]. Cr can also improve the oxidation resistance of steels [9]. A good strength–ductility combination can be achieved by adding V due to grain refinement strengthening and precipitation strengthening effects [10, 11]. Moreover, a reported research showed that the addition of 0.1% V in the Ni-Cr-Mo steel for brake discs significantly increased the thermal shock resistance and wear resistance [12]. The addition of Nb can effectively inhibit the grain growth due to solute drag effect and precipitate pinning effect [13, 14]. Nb can also retard the coarsening of $M_{23}C_6$ carbides and so improve the thermal fatigue performance of H13 steel [15]. However, there is little work focusing on the influence of Nb and higher V content on the performance of the steels used as brake discs. Therefore, a small amount of Nb and plenty of V are added to the Cr-Mo-V steel, and their influence on microstructural evolution is studied.

The austenite grain size has a great influence on the resultant microstructure and properties after heat treatment [16]. Grain refining can improve strength and toughness simultaneously. The reported researches showed that the sizes of martensite blocks and packets decreased with the refinement of austenite grains; therefore, both

*Corresponding author: Fuming Wang, School of Metallurgical and Ecological Engineering, University of Science and Technology Beijing, Beijing, China, E-mail: wangfuming@metall.ustb.edu.cn
Dan Wu: E-mail: bird5810761@163.com, Jin Cheng: E-mail: chengjin@ustb.edu.cn, School of Metallurgical and Ecological Engineering, University of Science and Technology Beijing, Beijing, China
http://orcid.org/0000-0003-0007-2429
Changrong Li, School of Materials Science and Engineering, University of Science and Technology Beijing, Beijing, China, E-mail: crli@mater.ustb.edu.cn

the yield strength and the impact energy increased [17, 18]. The austenitizing temperature and the holding time have great influence on the austenite grain size [10]. With increasing austenitizing temperature , more alloying elements are dissolved into matrix, and more carbides precipitate out in the subsequent tempering process, which improves the precipitation strengthening effect. However, the austenite grains are coarsening with increasing austenitizing temperature, and the grain refinement strengthening effect becomes weaker. In a sense, the grain refinement strengthening and the precipitation strengthening are contradictory. Moreover, the austenite transformation may occur under hard braking [3]. Therefore, it is necessary to study the austenite grain growth behavior of the Cr-Mo-V steel for brake discs.

In the present study, the grain growth behavior of the Cr-Mo-V steel with different vanadium and niobium contents was studied, and the influence of austenitizing temperature and alloying content on the precipitation behaviors was investigated based on transmission electron microscopy (TEM) and energy-dispersive spectroscopy (EDS) measurements. Moreover, the growth models of both the precipitates and the austenite grains were established, respectively. With a combination of calculation and measurement results, the relationship between the growth behaviors of the precipitates and the austenite grains was established theoretically. The results can provide a reference for the heat treatment process of the Cr-Mo-V steel for brake discs.

Experimental

The compositions of the tested steels with different vanadium and niobium contents are shown in Table 1. The thermo-Calc software package and the TCFE6 thermodynamic database were used to calculate the phase transition temperatures of the tested steels. The results are also shown in Table 1.

The schematic diagram of heat treatment processes is shown in Figure 1. The samples with a size of 10 mm × 10 mm × 10 mm were heated in a muffle furnace for 1 h at different temperatures (900, 950, 1,000, 1,050, 1,100 and 1,200 °C, respectively). Similarly, the samples were heated to 950 °C and held for different time periods (5, 15, 30 and 45 min, respectively). Then, the samples were quenched in water and the decarburization layer was removed. After being ground and polished, the samples were etched in the saturated aqueous picric acid solution (100 ml) with a little detergent (2–3 g shampoo) at 65 °C. The austenite grain morphologies of the tested steels were observed by an optical microscopy (OM, 9XB-PC), and the average austenite grain size was measured using the linear intercept method. For each sample, more than 400 intercepts were measured. The characteristics of precipitates, namely their morphology, size, quantity, distribution and chemical composition, were investigated using a TEM (JEM-2100F) and an EDS (Oxford X-Max). More than 300 precipitates were observed for each specimen.

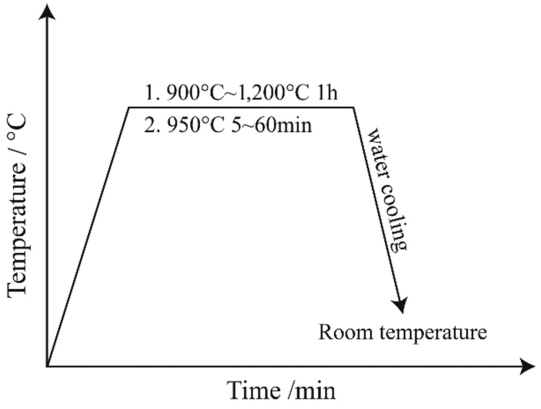

Figure 1: Schematic diagram of heat treatment processes of the tested steels.

Results and discussion

The growth behavior of austenite grains

Influence of austenitizing temperature on the grain growth behavior

The austenite grain morphologies and the average grain sizes of the tested steels quenched at different temperatures are shown in Figures 2 and 3, respectively. For steels A and

Table 1: The chemical compositions (mass %) and the phase transition temperatures (°C) of the tested steels.

Steels	C	Si	Mn	Cr	Ni	Mo	V	N	Nb	Fe	A_1 (°C)	A_3 (°C)
A	0.26	0.62	0.63	1.15	0.40	0.81	0.31	0.0031		Bal.	739	841
B	0.26	0.66	0.64	1.16	0.40	0.81	0.49	0.0027		Bal.	751	854
C	0.26	0.64	0.64	1.15	0.41	0.80	0.31	0.0025	0.045	Bal.	740	842

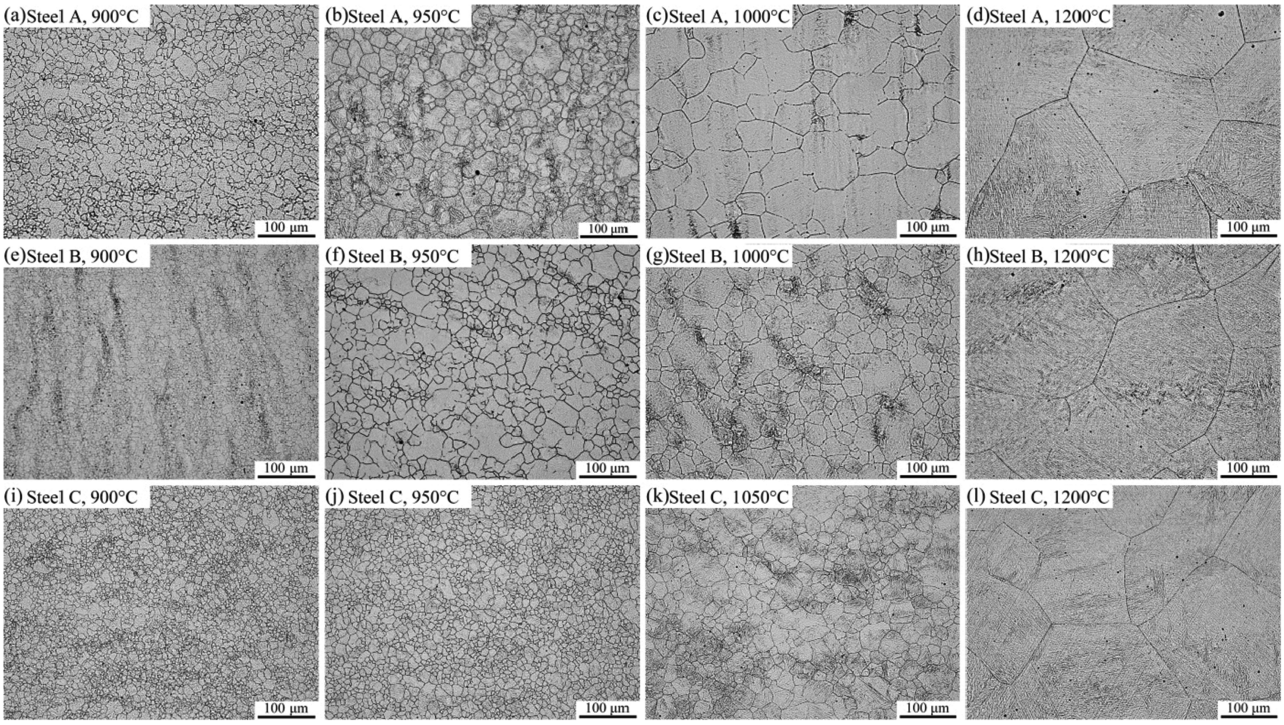

Figure 2: Austenite grain morphologies of the tested steels quenched at different temperatures for 1 h.

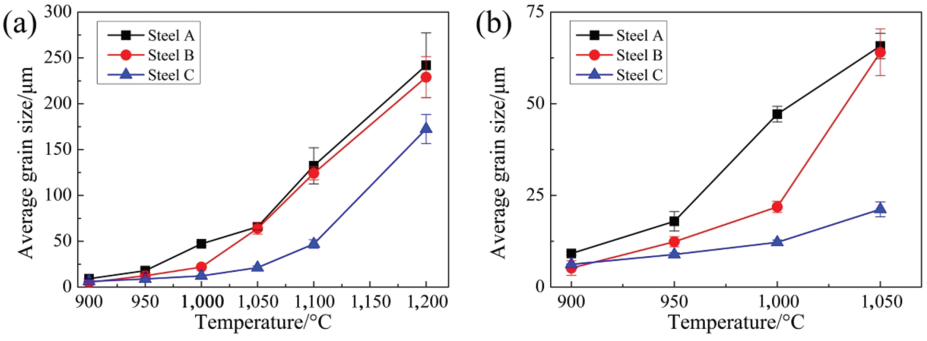

Figure 3: Effect of austenitizing temperature on the average grain sizes of the tested steels: (a) 900–1,200 °C; (b) 900–1,050 °C.

B, the grains grow rapidly with increasing temperature. The grains of steel B are smaller as compared to steel A when the temperature is below 1,000 °C, especially at 900 °C. However, there is no significant difference between the grains of the two Nb-free steels when the temperature is above 1,050 °C. Clearly, the grain refinement effect, which results from increasing V content, is only effective at lower temperatures. As for steel C, the grains grow slowly when the temperature is below 1,050 °C, and the average grain size is reduced from 242.0 ± 35.3 to 172.4 ± 16.0 μm with 0.045 % Nb addition when held at 1,200 °C, that is, the addition of Nb refines grains effectively at all experimental temperatures. Moreover, the additions of V and Nb increase the grain-coarsening temperature. The grain-coarsening temperatures of steels A, B and C are 950, 1,000 and 1,050 °C, respectively.

Moreover, the grains of steel A are not uniform in size when held at 950 °C (see Figure 2(b)), comprising of some abnormal coarse grains and fine grains, that is, the mixed grain phenomenon occurs. Compared with steel A, the grains of steel B are more inhomogeneous at 950 °C (see Figure 2(f)), indicating that the mixed grain phenomenon becomes more severe with increasing V content. Compared with the two Nb-free steels, the grains of steel C are smaller and more uniform in size (see Figure 2 (j)).

Influence of holding time on the grain growth behavior

The austenite grain morphologies and the average grain sizes of the tested steels quenched at 950 °C for different

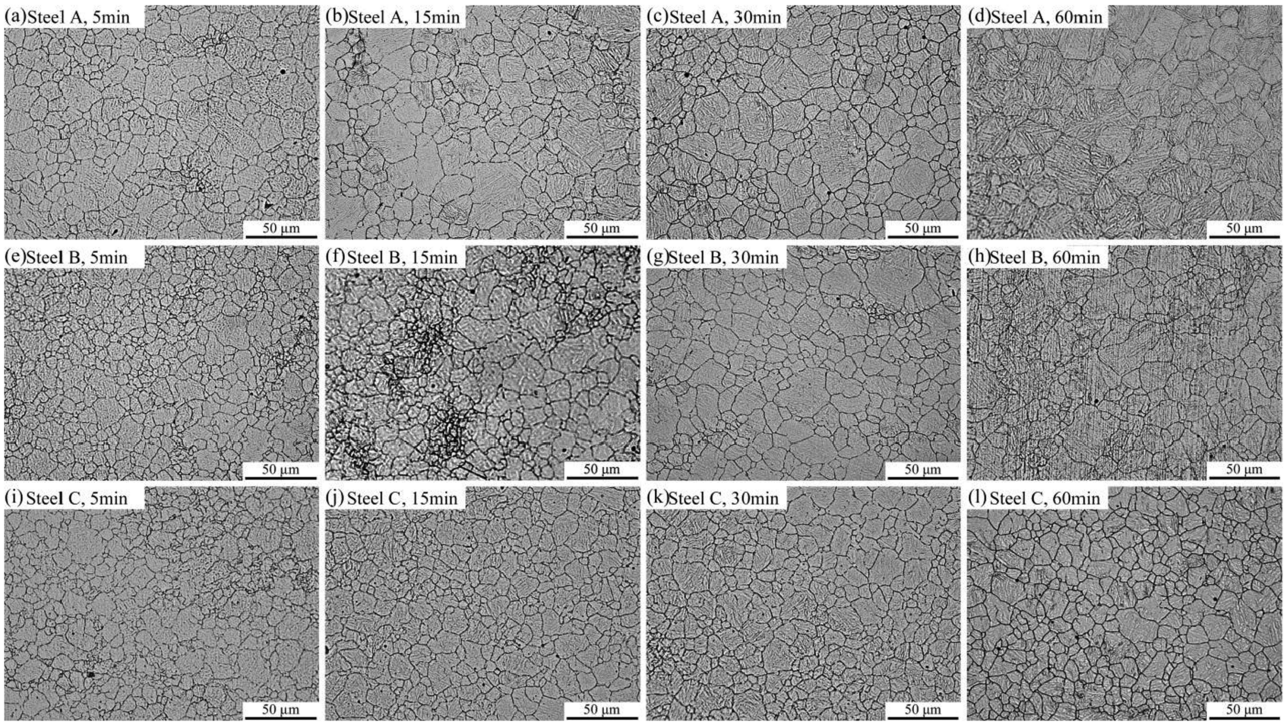

Figure 4: Austenite grain morphologies of the tested steels quenched at 950 °C for different holding times.

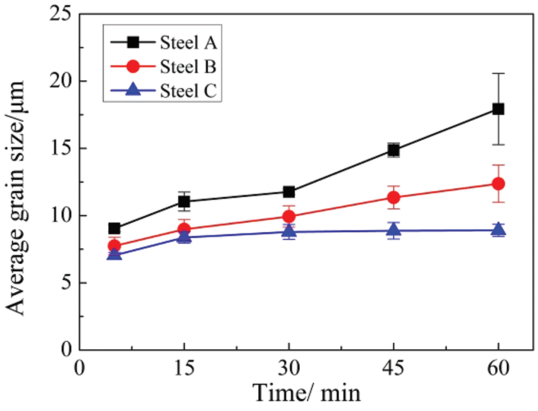

Figure 5: Effect of holding time on the average grain sizes of the tested steels.

holding times are shown in Figures 4 and 5, respectively. With prolonging holding time, the grains gradually grow and the number of small grains decreases. The grain growth rate of steel A is the fastest, next is that of steel B, and that of steel C is the slowest.

The grain growth trends in the tested steels are similar when the time is less than 30 min, but the growth rates are different above 30 min. For the two Nb-free steels, some abnormal coarse grains grow rapidly and the average grain sizes increase obviously above 30 min. The grains of steel B are smaller, but their size distribution becomes more uneven as compared to steel A. After long time holding, the precipitates are partially dissolved or coarsened; therefore, their pinning force decreases and results in a rapid grain growth [19]. Compared with the Nb-free steels, the grains of steel C are fine and more uniform in size, and the average grain size grows very slowly above 30 min, suggesting that the addition of Nb availably restrains the austenite grain growth.

Influence of the austenitizing temperature and the alloying elements on the precipitation behaviors of carbides and carbonitrides

Thermodynamic calculation

Thermo-Calc thermodynamic software package was used to calculate the precipitation behaviors of carbides and carbonitrides, as shown in Figure 6. The carbide-forming elements in steel A are Cr, Mo and V. The precipitation temperatures of $M_{23}C_6$, MC and M_7C_3 carbides are lower than the experimental temperatures and so the carbides are dissolved during heating. There are some undissolved V(C, N) particles that exist at the experimental temperatures

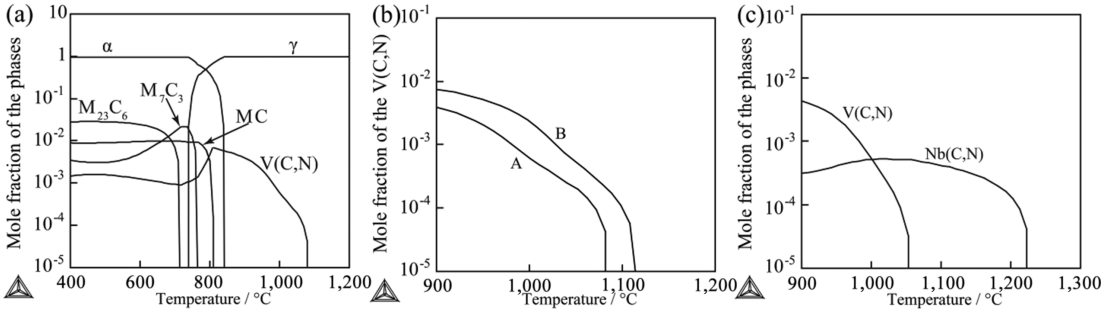

Figure 6: Precipitation behaviors in (a) steel A at 400–1,200 °C; (b) steels A and B at 900–1,200 °C; (c) steel C at 900–1,200 °C.

due to its high precipitation temperature. Moreover, Nb(C, N) particles exist in steel C (see Figure 6(c)). These undissolved carbonitrides can restrain the grain growth.

The V content has a great influence on the precipitation behavior of V(C, N) particles. By increasing the V content from 0.31 % to 0.49 %, the precipitation temperature is increased from 1,080 to 1,120 °C and the amount of precipitates is also increased obviously. Therefore, the grain refinement effect is more effective in steel B, especially at 900 °C. However, the amount of V(C, N) decreases rapidly and the refinement effect becomes weaker with increasing temperature. Therefore, the difference between the grain sizes of the two Nb-free steels is not obvious at higher temperatures. For steel C, both V(C, N) and NbC precipitate at the experimental temperatures, and their precipitation temperatures are 1,050 °C and 1,220 °C, respectively. The precipitation behavior of V(C, N) is similar to that of the other two steels. Since NbC is more stable than VC, its refinement effect is still evident when the temperature is above 1,050 °C. Therefore, the average grain size of steel C is obviously reduced.

Influence of the austenitizing temperature on the precipitation behaviors of carbides and carbonitrides

The morphologies, diffraction patterns and EDS analyses of the precipitates in steel A with different austenitizing temperatures are shown in Figure 7. There are some round-shaped precipitates in the steel, which can be identified as V-rich M_8C_7 according to the diffraction patterns and EDS analyses.

As mentioned above, some grains of steel A grow abnormally at 950 °C, that is, the mixed grain phenomenon occurs. In order to explain this phenomenon, the characteristics of precipitates, including morphology and size distribution, were investigated in the samples of steel A, as shown in Figure 8. By increasing the temperature

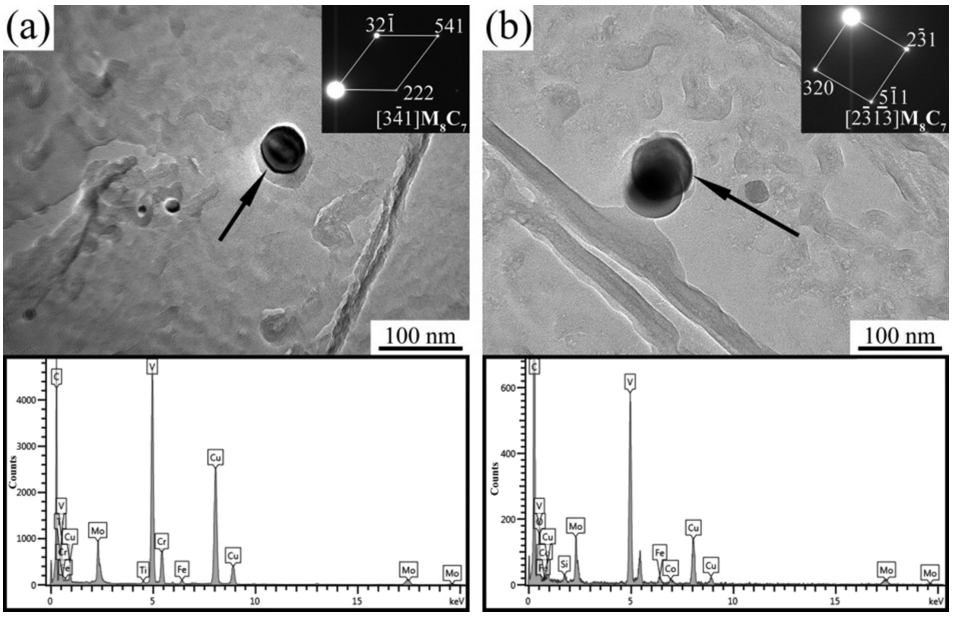

Figure 7: TEM micrographs, diffraction patterns and EDS analyses of the precipitates in steel A quenched at (a) 900 °C and (b) 950 °C.

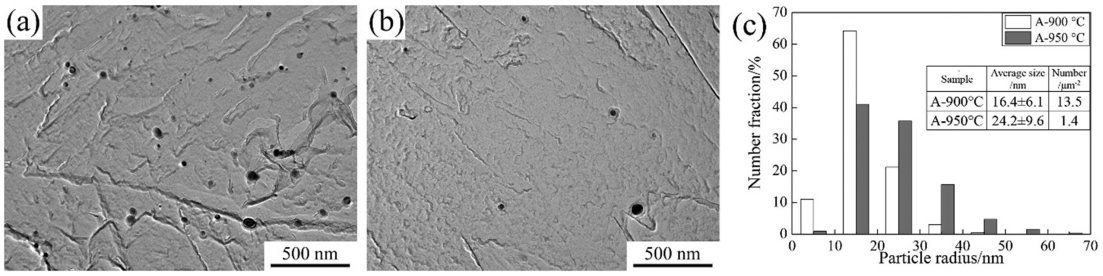

Figure 8: Morphologies and size distributions of the precipitates in steel A: (a) quenched at 900 °C; (b) quenched at 950 °C; (c) size distributions.

from 900 to 950 °C, the precipitates are dissolved and coarsened, and the statistical results show that the average size of precipitates is increased from 16.4 ± 6.1 to 24.2 ± 9.6 nm and their amount is reduced from 13.5 to 1.4 μm^{-2}, so their refinement effect is dramatically reduced. Moreover, the precipitates may be mostly dissolved in some areas and the pinning force decreases [20]. The grains in the area with poor pinning force will grow fast, while the growth of normal grains is suppressed. Therefore, the mixed grain phenomenon occurs.

Influence of alloying elements on the precipitation behaviors of carbides and carbonitrides

As shown in Figure 9, there are some round- or oval-shaped precipitates in steels B and C. V-rich M_8C_7 particles exist in both steels B and C, and a little Nb is detected in M_8C_7 particles in steel C due to the addition of Nb. Moreover, NbC carbides are observed in steel C.

Figure 10 shows the morphologies and the size distributions of the precipitates in the tested steels quenched at 950 °C. The amount of M_8C_7 particles increases obviously with increasing V content, which is 10.1 μm^{-2} in steel B. However, the precipitate distribution becomes heterogeneous with increasing V content. The larger precipitates tend to gather together, and so do the smaller precipitates (see Figures 10(b)). The uneven distribution of precipitates leads to a difference of pinning force in different areas, causing the mixed grain phenomenon to be more severe in steel B as compared to steel A (see Figures 2(b) and (f)). Moreover, the average sizes of M_8C_7 particles do not change much with increasing V content, which are 24.2 ± 9.6 and 25.5 ± 9.8 nm in steels A and B, respectively.

Compared with steel A, the amount of small precipitates significantly increases in steel C. The statistical results show that the average size of precipitates is reduced to 12.7 ± 7.7 nm and their amount is increased to 18.4 μm^{-2}. These small precipitates, which are mainly NbC, are evenly dispersed and provide a significant pinning effect (see

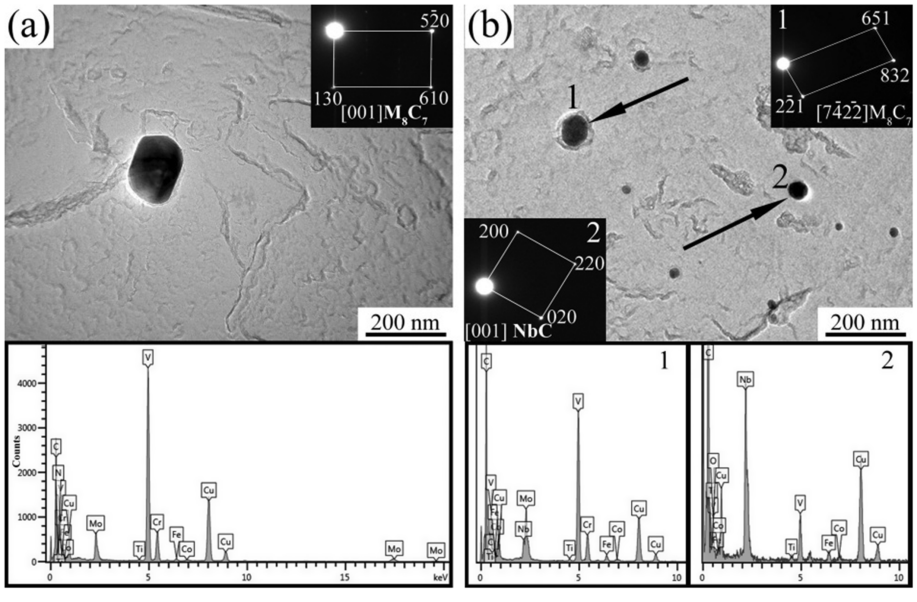

Figure 9: TEM micrographs, diffraction patterns and EDS analyses of the precipitates quenched at 950 °C in (a) steel B and (b) steel C.

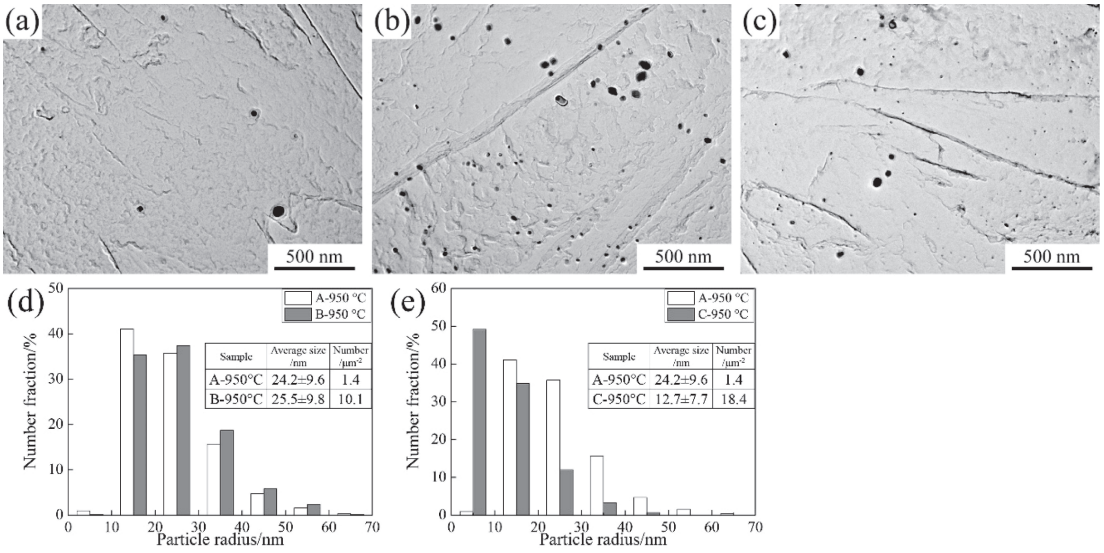

Figure 10: Morphologies of the precipitates quenched at 950 °C: (a) steel A; (b) steel B; (c) steel C and size distributions of the precipitates: (d) steels A and B; (e) steels A and C.

Figure 2(j)). Therefore, the grains of steel C grow slowly with increasing temperature and holding time. Moreover, the amount of large precipitates, which are mainly M_8C_7, changes little in steel C as compared to steel A.

Growth models of precipitates and austenite grains

During heating and soaking processes, Ostwald ripening will occur, that is, small particles dissolve and large particles coarsen. Since nitrogen contents in the tested steels are low, the precipitates are mainly VC and NbC. Lifshitz and Slyozov studied the kinetic equation of precipitate coarsening [21]:

$$r^3 - r_0^3 = \frac{8 \cdot \sigma \cdot V \cdot D \cdot t \cdot C^s}{9 \cdot R \cdot T} \quad (1)$$

where r and r_0 are the final and initial particle radius (cm), respectively, σ is the interfacial energy, V is the molar volume ($V_{NbC} = 13.75$ cm^3/mol, $V_{VC} = 11.31$ cm^3/mol) [22], D is the diffusivity of solute atom in matrix (cm^2/s), t is the coarsening time (s), C^s is the concentration of solute atom in matrix (mass %), which is calculated by Thermo-Calc software, R is the universal gas constant (8.31 J/mol·K^{-1}), T is the austenitizing temperature (K).

The interfacial energies of NbC and VC [22] in austenite are given as:

$$\sigma_{NbC-\gamma} = 1.3434 - 0.6054 \times 10^{-3} T \quad (2)$$

$$\sigma_{VC-\gamma} = 1.1292 - 0.5088 \times 10^{-3} T \quad (3)$$

The diffusivities of Nb and V [22] in austenite are given as:

$$D_{Nb} = 0.83 \times \exp(-266500/RT) \quad (4)$$

$$D_V = 0.28 \times \exp(-264000/RT) \quad (5)$$

The TEM results show that some particles have a radius of 5–10 nm in the tested steels, so the initial particle radius (r_o) is assumed as 5×10^{-7} cm. The solubilities of Nb and V are shown in Figure 11. The coarsening time is 3,600 s. Substituting corresponding numerical values into eq. (1), the final particle radii at different temperatures were calculated, and the results are shown in Figure 12.

The growth of the precipitates is all in a parabolic way in the tested steels. With increasing temperature, the average size of M_8C_7 particles obviously increases and their pinning effect becomes weaker, so the grain sizes of the two Nb-free steels change obviously. The average size of NbC is much less than that of VC. Therefore, there are many small precipitates and the average size of precipitates is significantly reduced with Nb addition (see Figure 10(c), (e)). Moreover, the coarsening rate of VC slightly increases with increasing V content, but it changes little with Nb addition, which are consistent with the measured results (see Figure 10 (c), (d)).

VC particles are continuously dissolved with increasing temperature (see Figure 6). At lower temperatures, the amount of VC is large and so the pinning effect is very strong. But when the temperature is above 1,050 °C, the pinning effect of VC becomes weaker due to its rapid coarsening and almost complete dissolution. As for NbC,

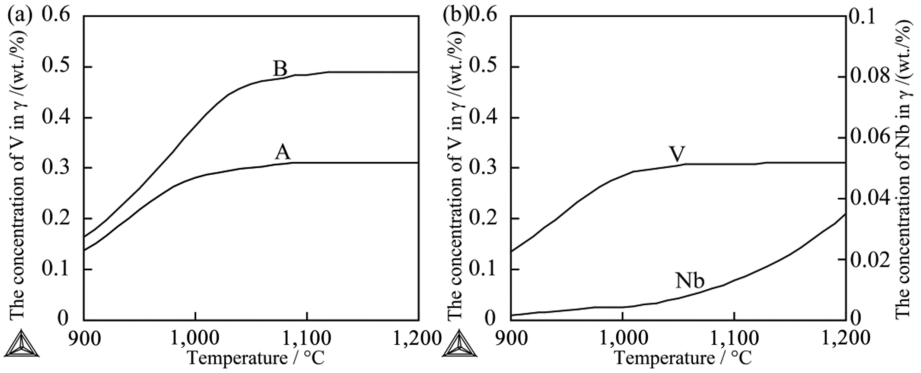

Figure 11: The concentrations of solute atoms in (a) steels A and B and (b) steel C.

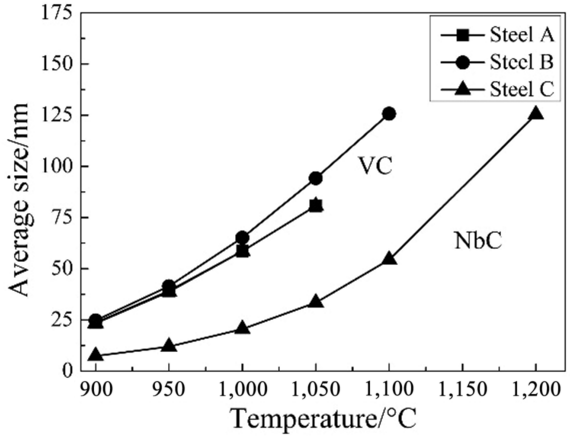

Figure 12: The calculated radii of VC and NbC particles in the tested steels at different temperatures.

its amount keeps stable in a large temperature range and its coarsening rate is much slower than that of VC. Therefore, NbC is chosen to predict the critical grain size.

Zener [23] first proposed the basic principle of austenite grain coarsening, which was according to the balance of the grain growth force and the pinning force of precipitates. Hillert [24] proposed that normal grain growth and abnormal grain growth are at two growth limits. Gladman [25] considered the energy change caused by grain boundary movement and gave the expression of the critical grain size (R_c):

$$R_c = [\pi(1/4 - 1/3Z)]r/f \tag{6}$$

where Z is the inhomogeneity factor of grain size (the ratio of the maximum grain radius to the average grain radius). In general, metal material Z = 1.7 [26], so the critical grain diameter (D_c) can be given as:

$$D_c = 2R_c = 0.34 \cdot r/f \tag{7}$$

For NbC particles, the volume fraction (f) in steel is:

$$f = (M - [M])\frac{A_M + xA_X}{A_M}\frac{d_{Fe}}{100d_{MX}} \tag{8}$$

where M is the content of M element in steel (0.045 %), $[M]$ is the equilibrium concentration of solute atom which is the same as C^s in eq. (1), A_M and A_X are the atomic weights of M and X ($A_{Nb} = 92.91$, $A_C = 12.01$), respectively, d_{Fe} and d_{MX} are the densities of iron matrix and precipitate ($d_{Fe} = 7.87 \times 10^3$ mg·cm^{-3}, $d_{NbC} = 7.803 \times 10^3$ mg·cm^{-3}) [22], respectively, $x$is the atomic ratio of M to X in MX($x = 1$). Substituting corresponding numerical values into eq. (7) and eq. (8), the measured and calculated diameters of grains and the volume fraction of NbC in steel C were calculated, as shown in Figure 13.

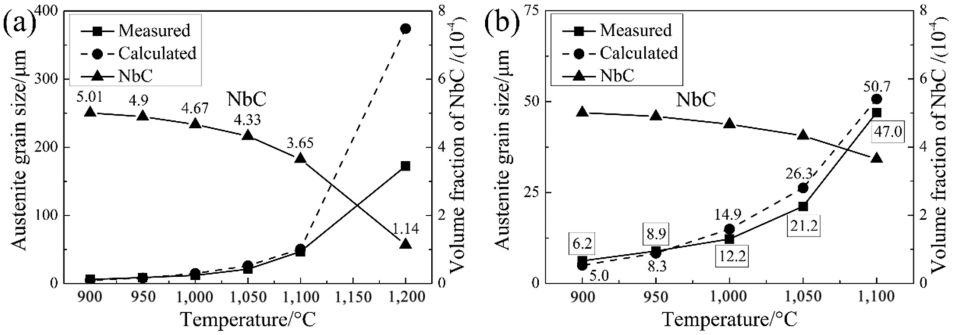

Figure 13: The measured and calculated diameters of austenite grains and the volume fraction of NbC in steel C at: (a) 900–1,200 °C; (b) 900–1,100 °C.

When the temperature is below 1,100 °C, the volume fraction of NbC decreases slowly, and the difference between the calculation and the measurement results is not significant. The calculated diameters are slightly larger than the measurement diameters in the temperature range of 1,000–1,100 °C, which should be caused by the solute drag effect of Nb [13]. With increasing temperature, the concentration of solute Nb increases and its solute drag effect becomes stronger [27], so the grains are slightly refined. However, the difference between the calculation and the measurement results is large at 1,200 °C. With increasing the temperature from 1,100 to 1,200 °C, the average radius of NbC increases from 54.4 to 125.3 nm and its volume fraction reduces from 3.65×10^{-4} to 1.14×10^{-4}, so the pinning effect of NbC becomes weaker and it will be inaccurate to predict the grain size by use of this model.

Conclusions

The Cr-Mo-V steel for brake discs is a low alloy quenched and tempered steel, which is sensitive to the change of austenitizing parameters. Therefore, the grain growth behavior of the steel with different vanadium and niobium contents was studied. The major results are summarized as follows:

(1) V-rich M_8C_7 particles are observed in the Nb-free steels after a quenching process, while both M_8C_7 and NbC particles exist in the Nb-bearing steel. The carbides of Mo and Cr are dissolved in the austenitizing process. The experimental results are consistent with the thermodynamic calculation results.

(2) The abnormal grain growth behavior occurs in the Nb-free steels at 950 °C, which is affected by the partial dissolution and coarsening of M_8C_7 particles, and so the austenitizing temperature should be lower than 950 °C. The grain size decreases with increasing V content, but the precipitate distribution becomes more heterogeneous, aggravating the mixed grain phenomenon. For the Nb-bearing steel, many small NbC particles precipitate, so the grain refinement effect is significant.

(3) The growth models of precipitates and austenite grains are established. The grain growth model is well consistent with the actual situation in the Nb-bearing steel up to 1,100 °C. However, the difference between the calculation results and the experimental measurement becomes distinct at 1,200 °C due to the large dissolution and sharply coarsening of NbC particles. For the Nb-free steels, M_8C_7 particles dissolve or coarsen rapidly with increasing temperature, causing the obvious increase of the grain size.

Funding: This work was supported by the National Natural Science Foundation of China (Grant No. 51674020).

References

[1] Z. Yang, J. Han and W. Li, Eng. Fail. Anal., 34 (2013) 121–128.
[2] Z.Y. Yang, Z.Q. Li and Y. Chen, Adv. Mater. Res., 314 (2011) 1135–1141.
[3] Z. Li, J. Han and Z. Yang, Eng. Fail. Anal., 57 (2015) 202–218.
[4] Z. Li, J. Han, Z. Yang and L. Pan, Eng. Fail. Anal., 44 (2014) 272–284.
[5] C.H. Gao, J.M. Huang, X.Z. Lin and X.S. Tang, J. Tribol., 129 (2007) 536–543.
[6] J.S. Li, H.P. Li, B.Q. Jiao, B.J. Lv, D.F. Chen and L.L. Gu, Appl. Mech. Mater., 419 (2013) 370–375.
[7] Z. Li, J. Han, W. Li and L. Pan, Mater. Des., 56 (2014) 146–157.
[8] H.J. Jun, J.S. Kang and D.H. Seo, Mater. Sci. Eng., 422 (2006) 157–162.
[9] N.J. Simms and J.A. Little, Oxid Met, 27 (1987) 283–299.
[10] R. Staśko, H. Adrian and A. Adrian, Mater. Charact, 56 (2006) 340–347.
[11] D. Wu, F. Xiao and B. Wang, Mater. Sci. Eng., 592 (2014) 102–110.
[12] N. Harada, M. Takuma and M. Tsujikawa, Wear, 302 (2013) 1444–1452.
[13] L.M. Fu, H.R. Wang and W. Wang, Mater. Sci. Technol., 27 (2011) 996–1001.
[14] K.A. Annan, C.W. Siyasiya and W.E. Stumpf, J. S. Afr. Inst. Min. Metall., 115 (2015) 973–980.
[15] X. Hu, L. Li, X. Wu and M. Zhang, Int J Fatigue, 28 (2006) 175–182.
[16] M. Maalekian, R. Radis and M. Militzer, Acta Mater, 60 (2012) 1015–1026.
[17] Y. Prawoto, N. Jasmawati and K. Sumeru, J. Mater. Sci. Technol., 28 (2012) 461–466.
[18] C. Wang, M. Wang, J. Shi, W. Hui and H. Dong, J. Mater. Sci. Technol., 23 (2007) 659–664.
[19] S.F. Tao, F.M. Wang, G.L. Sun, Z.B. Yang and C.R. Li, Metall. Mater. Trans., 46 (2015) 3670–3678.
[20] P.R. Rios, Scr. Mater., 38 (1998) 1359–1364.
[21] I.M. Lifschitz and V.V. Slyozov, J. Phys. Chem. Solids, 19 1961 35–50.
[22] Q.L. Yong, Second Phases in Structural Steel, Metallurgical Industry Press., Beijing (2006).
[23] C. Zener, Trans. AIME, 175 (1949) 15–51.
[24] M. HILLERT, Acta Metal, 13 (1965) 227–238.
[25] T. Gladman and F.B. Pickering, J. Iron Steel Inst., 205 (1967) 653–664.
[26] N.E. Hannerz and F.D.E. Kazinczy, J. Iron Steel Inst., 208 (1970) 475–481.
[27] A. Karmakar, S. Kundu, S. Roy, S. Neogy, D. Srivastav and D. Chakrabarti, Mater. Sci. Technol., 30 (2014) 653–664.